

Acta Medica Okayama

Volume 43, Issue 2

1989

Article 6

APRIL 1989

Initiation and recovery processes of endotoxin
induced disseminated intravascular
coagulation (DIC): scanning and transmission
electron microscopic observations of rat renal
tissues.

Takanao Miyashima*

Keiki Hayashi†

Michiyasu Awai‡

*Okayama University,

†Okayama University,

‡Okayama University,

Initiation and recovery processes of endotoxin induced disseminated intravascular coagulation (DIC): scanning and transmission electron microscopic observations of rat renal tissues.*

Takanao Miyashima, Keiki Hayashi, and Michiyasu Awai

Abstract

To clarify the initiation, development and recovery processes of disseminated intravascular coagulation (DIC), rat glomerular capillaries and fibrin thrombi were examined under transmission and scanning electron microscopes. DIC was induced in rats by a single intraperitoneal injection of endotoxin (Et., 7.5 mg/kg lipopolysaccharide:B, E. coli 026:B6). At 2 h after Et. injection, the endothelial surface of the glomerular capillary became irregular with projections like a sea anemone. At 4 h after Et. injection, agglomerated fibrin thrombi composed of fibrin fiber bundles with fine cross-striated fibriform structures were observed in the capillary lumen. The fibrin thrombi gradually changed into fine reticular systems suggesting a degradation process by 6 h after Et. injection, and formed a coarse granular agglomerate by 8 h after Et. injection. These fibrin thrombi disappeared within 12 h of Et. injection, but the endothelial surface remained edematous. At 24 h after Et. injection, the microstructure of the glomerular capillaries returned normal. Based on these observations, we concluded that DIC was primarily initiated by injury to the capillary endothelium, and that changes on the endothelial surface contributed to the development of DIC.

KEYWORDS: disseminated intravascular coagulation, renal tissue, electron microscope, rat

*PMID: 2728905 [PubMed - indexed for MEDLINE]

Copyright (C) OKAYAMA UNIVERSITY MEDICAL SCHOOL

Initiation and Recovery Processes of Endotoxin Induced Disseminated Intravascular Coagulation (DIC): Scanning and Transmission Electron Microscopic Observations of Rat Renal Tissues.

Takanao Miyashima *, Keiki Hayashi and Michiyasu Awai

First Department of Pathology, Okayama University Medical School, Okayama 700, Japan

To clarify the initiation, development and recovery processes of disseminated intravascular coagulation (DIC), rat glomerular capillaries and fibrin thrombi were examined under transmission and scanning electron microscopes. DIC was induced in rats by a single intraperitoneal injection of endotoxin (Et., 7.5 mg/kg lipopolysaccharide : B, *E. coli* 026 : B6). At 2 h after Et. injection, the endothelial surface of the glomerular capillary became irregular with projections like a sea anemone. At 4 h after Et. injection, agglomerated fibrin thrombi composed of fibrin fiber bundles with fine cross-striated fibriform structures were observed in the capillary lumen. The fibrin thrombi gradually changed into fine reticular systems suggesting a degradation process by 6 h after Et. injection, and formed a coarse granular agglomerate by 8 h after Et. injection. These fibrin thrombi disappeared within 12 h of Et. injection, but the endothelial surface remained edematous. At 24 h after Et. injection, the microstructure of the glomerular capillaries returned normal. Based on these observations, we concluded that DIC was primarily initiated by injury to the capillary endothelium, and that changes on the endothelial surface contributed to the development of DIC.

Key words : disseminated intravascular coagulation, renal tissue, electron microscope, rat

Disseminated intravascular coagulation (DIC) is an acute clinical entity (1-3) with abnormal clotting and fibrinolysis resulting in multiple organ failure. Recently, chronic DIC (4), local DIC (5) and compensated DIC (6, 7) entities have been proposed. Pathological criteria of these entities have not yet been decided upon because: (a) DIC is followed by various diseases of diverse etiologies, (b) the profiles of symptom vary, (c)

the clotting and fibrinolysis vary according to the severity and stage of DIC and (d) differences exist in the initiation mechanism (1). Margaretten (8) emphasized the importance of tissue thromboplastin released by damaged endothelium as the initiation trigger of DIC, but platelet factor IX was proposed by Lipinski and Jeljaszewicz (9), prekallikrein (Fletcher factor) by Hathaway *et al.* (10) and kininogen (Fitzgerald factor) by Saito *et al.* (11). Vassalli *et al.* (12) and Bleyl (13) studied the ultramicrostructure of renal

* To whom correspondence should be addressed.

tissues in DIC using the transmission electron microscope. However, to date there has been no meticulous ultramicrostructural study on the relationship between fibrin thrombi and the glomerular capillary during DIC. In the present transmission and scanning electron microscopic study, we clarify the changes in the glomerular endothelium and fibrin thrombus during the initiation, development and degradation of endotoxin induced DIC.

Materials and Methods

Animals and procedures. Two hundred and ten male Wistar rats weighing 250-300 g were used. Fifty-seven animals were used to determine the LD₅₀ for endotoxin (Et.). Et. at 100 mg (Lipopolysaccharide : B, *E. coli* 026 : B6, Difco Labs., Detroit, MI, USA) was dissolved in sterilized physiologic saline (20 ml) immediately before use. A dose of 1, 2.5, 5, 7.5, 10 or 15 mg/kg was intraperitoneally injected with a 27 G needle into each animal under ether anesthesia.

One hundred fifty-three animals were divided into two groups: Group A (125 animals) received 7.5 mg/kg Et. as the DIC model (14) and group B (28 animals) received an injection of sterilized physiologic saline as the control. All animals were kept on a standard animal diet (Oriental Co., Osaka, Japan) and received water *ad libitum*. They were acclimatized for one week prior to the experiment at 22-25°C. During the experiment, they were kept in metabolic cages for urine collection. Five animals in group A without symptoms of DIC (*i.e.* hematuria, oliguria, bleeding tendency) and without a fibrin thrombus in the glomerulus, and 51 other animals that died before sacrifice, were excluded from the study.

In group A, 6 animals each were sacrificed at 1, 2, 4, 8, 12, 18, 24, 36, 48 and 72 h after injection, and in group B, 4 animals each were sacrificed at 0, 2, 4, 12, 24, 48 and 72 h after injection. Urinalysis was conducted on hourly urine collections.

At sacrifice, the abdominal wall was incised after an intraperitoneal injection of Nembutal (20 mg/kg). A teflon catheter connected to a syringe

without an anticoagulant was inserted into the abdominal aorta, and 4 ml of blood was withdrawn for hematological analyses. Immediately after this withdrawal, the left renal artery and vein were ligated and the left kidney was rapidly removed. A part of the renal tissue was fixed in 2% buffered glutaraldehyde for the specimens of transmission electron microscope (TEM), and the remainder was fixed in 10% buffered formalin for the light microscope specimens. In the remaining nephrectomized animals, the aorta was ligated at the upper portion of the diaphragm, and sterilized physiological saline (4°C) was perfused for 2 min at a pressure of 50 cmH₂O. Perfusion fixation was performed with 1% glutaraldehyde in 0.3 M phosphate buffer (pH 7.3, 4°C) at the same pressure for 10 min for the specimens of scanning electron microscope (SEM).

Hematological and urinary analyses. A part of the blood sample was used for the platelet count and measurement of fibrinogen degradation products (FDP). One-tenth volume of 3.8% sodium citrate was added to the remainder and centrifuged (3000 rpm, for 15 min) to collect the plasma for measuring fibrinogen. Platelets were counted by an automated thrombocounter (Toa Co., Kobe, Japan). Plasma FDP values were converted to human fibrinogen values ($\mu\text{g/ml}$) using the latex aggregation reaction test (FDPL test, Teikoku Hormone Mfg. Co., Tokyo, Japan; minimum detection level, 1 $\mu\text{g/ml}$). Plasma fibrinogen values were determined by the thrombin coagulation method (Fibrinogen measurement reagent, American Dade Co., Florida, USA). Urinary FDP values were determined using the latex aggregation reaction test (FDPL test-U, Teikoku Hormone Mfg. Co.; minimum detection level, 0.2 $\mu\text{g/ml}$), and converted to human fibrinogen ($\mu\text{g/ml}$) equivalents.

Histochemical procedures. After 2 days fixation in 10% buffered formalin, the renal tissues were embedded in paraffin, cut into 5 sections of 4 μm each, stained with hematoxylin and eosin (HE) and phosphotungstic acid hematoxylin (PTAH), and reacted to antibodies of anti-rat fibrinogen, anti-human FDP-D and FDP-E by the avidin biotin complex (ABC) method (15, 16). DIC animals were defined as those with fibrin thrombi in more than 20% of the loops of the examined glomeruli (14).

TEM procedures. Rat renal tissues cut into

1-mm³ blocks were fixed in 2% glutaraldehyde (buffered to pH 7.4 with 0.1 M PBS) at 4°C for 2 h, washed 2 times in PBS, dehydrated in a graded ethanol series (50-100%), and embedded in Ladd low viscosity resin kit (Spur Kit) at 45°C for 2 h, 60°C for 2 h and 70°C for 14 h. Ultrathin sections were cut with an ultramicrotome (Sorvall Co. MT-5000), dipped in a mesh (Veco-150), doubly stained with uranyl acetate and lead citrate and examined under a TEM (H-600) at 80 kV.

SEM procedures. The right kidney removed after perfusion-fixation was cut into 5 mm×3 mm×3 mm blocks, fixed by the same method as for TEM and post-fixed in 2% tannic acid (diluted in 0.1 M PBS) at 4°C for 6 h. After repeating the osmium tetroxide and tannic acid procedures 3 times, the specimens were washed 3 times in PBS, and dehydrated in a graded ethanol series (20-100%). Specimens were freeze-cracked in liquid nitrogen, transferred to an isoamylacetate series, processed by CO₂ critical point drying with an HCP-2 Critical Point Dry System, vacuum-evaporated with white gold with a IB-3 Ion Coating System (Eiko Engineering Co., Ibaragi, Japan) and examined with a SEM (S-430) at 20 kV.

Results

Et. dose dependence. Table 1 shows the relationship between the Et. dose and rat mortality 10 h after Et. injection. All animals survived at 1 mg/kg, 7 of 13 (53.8%) died at 7.5 mg/kg, and all died at 15 mg/kg. The table also shows the relationship between the Et. dose and fibrin thrombi in the glomeruli at 6 h after Et. injection. When an animal died before 6 h, the renal tissues

were examined upon death. No fibrin thrombus was observed at 1 mg/kg. Fibrin thrombi were found in only 1 of 6 (16.7%) animals at 15 mg/kg, but were found in 7 of 8 (87.5%) animals at 7.5 mg/kg. Animals injected with a heavy dose of Et. (more than 10 mg/kg) tended to die earlier (immediately after or within 1 h of the Et. injection). A dose of 7.5 mg/kg Et. was the LD₅₀.

Hematological and biochemical analyses. Fig. 1 shows the platelet counts of group A and B rats. In group A, the platelet count decreased immediately after Et. injection, reached a minimum at 4 to 6 h, gradually increased and returned to the normal level at 72 h.

Fig. 2 shows the serum fibrinogen and FDP values of group A rats. After Et. injection, fibrinogen values decreased at 2 h, reached a minimum at 4 to 6 h, then gradually increased and returned to the normal level at 72 h. On the other hand, serum FDP appeared at 4 h, increased rapidly, reached a maximum at 6 h, then rapidly decreased and disappeared by 24 h after Et. injection.

Fig. 3 shows the urinary FDP values of group A and B rats. In group A, urinary FDP increased rapidly by 4 h after Et. injection, reached a maximum by 8 h, then decreased rapidly and disappeared by 18 h.

Fig. 4 shows the urinary volume of group A and B rats. After Et. injection, oliguria began by 1 h, near anuria continued from 4 to 6 h, mild diuresis started at 6 h and the volume returned to normal at 36 h.

Table 1 Rat mortality and fibrin thrombus in the glomerulus after endotoxin injection

Endotoxin (mg/kg)	1	2.5	5	7.5	10	15
Animal death ^a	0/8 (0%)	1/8 (12.5%)	3/9 (33.3%)	7/13 (53.8%)	9/10 (90%)	9/9 (100%)
Fibrin thrombus in glomerulus ^b	0/8 (0%)	1/8 (12.5%)	3/9 (33.3%)	7/8 (87.5%)	4/10 (40%)	1/6 (16.7%)

a: Within 10 h of endotoxin injection.

b: Six hours after Et. injection or upon death.

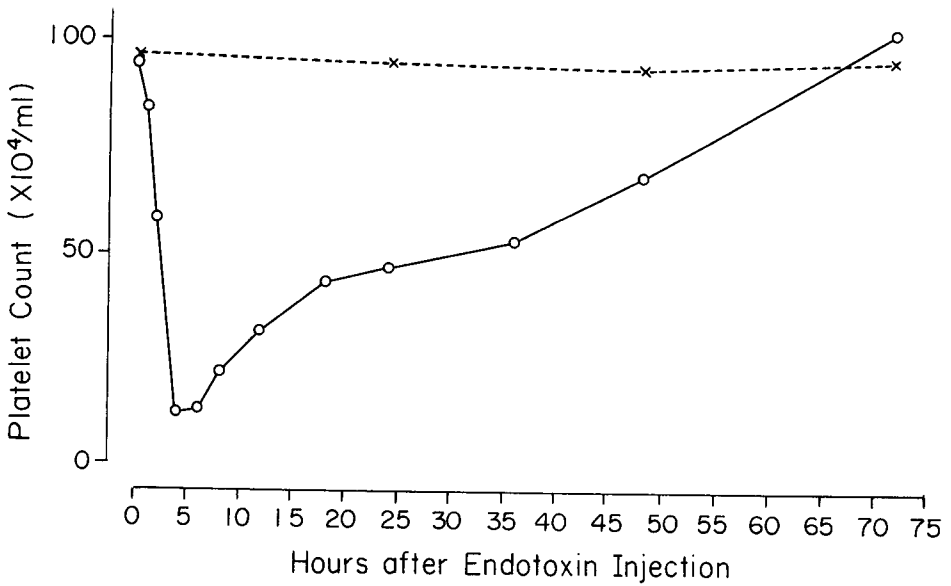


Fig. 1 Platelet count after injection of endotoxin (Et., 7.5 mg/kg) or saline. O, Et.-injected rats (n = 6). X, Saline injected rats (n = 4).

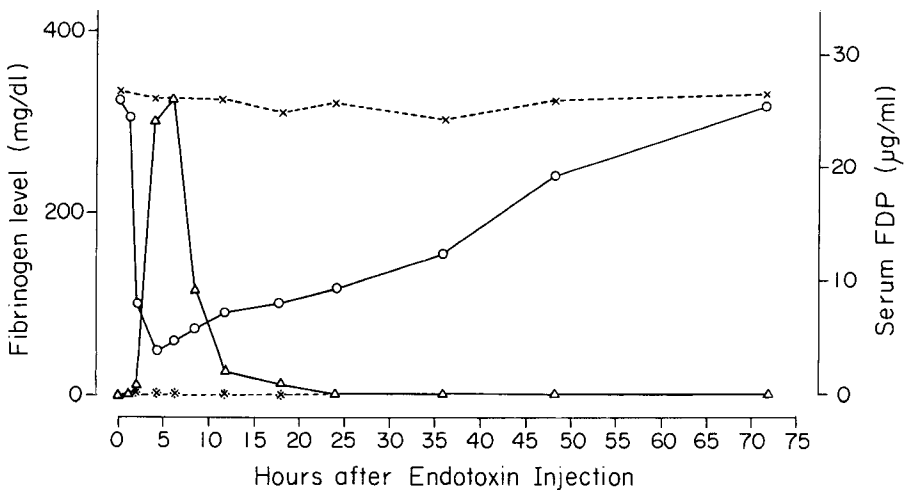


Fig. 2 Serum fibrinogen and FDP values after injection of endotoxin (Et., 7.5 mg/kg) or saline. O, Fibrinogen values of Et.-injected rats (n = 6). Δ, FDP values of Et.-injected rats (n = 6). X, Fibrinogen values of saline-injected rats (n = 4). *, FDP was not detected in saline-injected rats (n = 4).

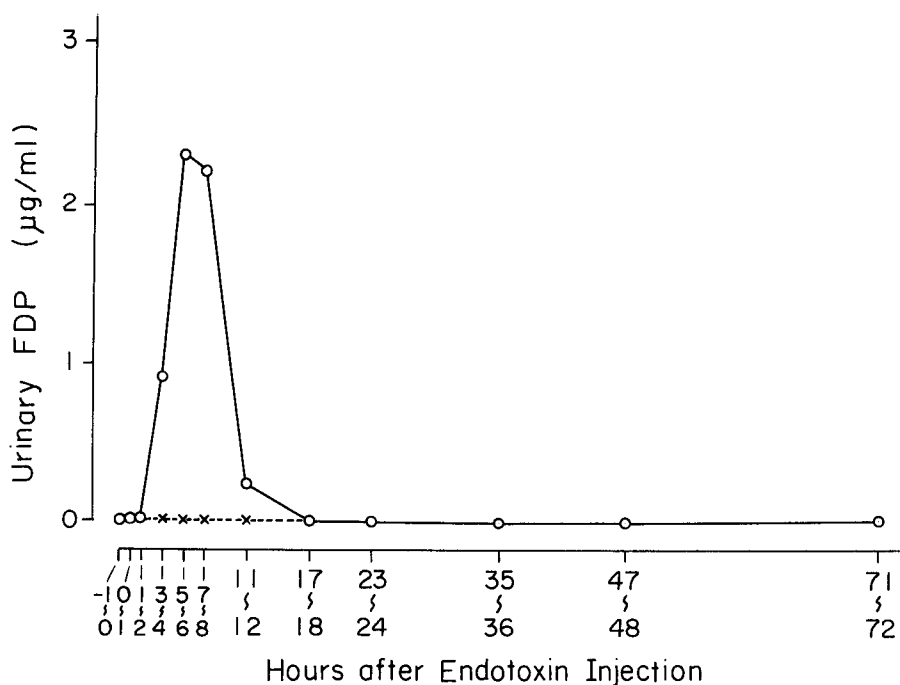


Fig. 3 Urinary FDP values after injection of endotoxin (Et., 7.5 mg/kg) or saline. O, Et.-injected rats (n = 4). X, FDP was not detected in saline-injected rats (n = 4).

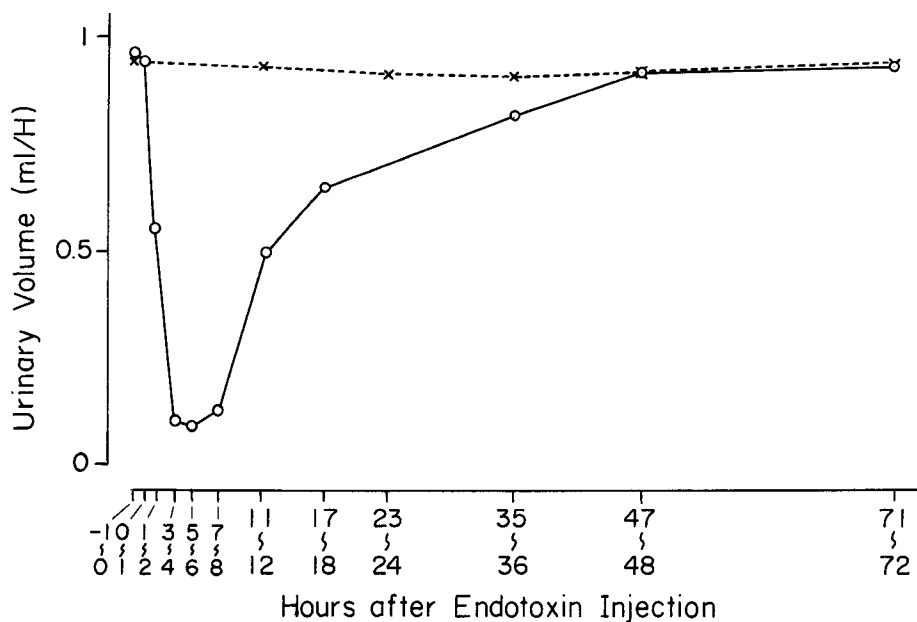


Fig. 4 Urinary volume after injection of endotoxin (Et., 7.5 mg/kg) or saline. O, Et.-injected rats (n = 6). X, Saline-injected rats (n = 4).

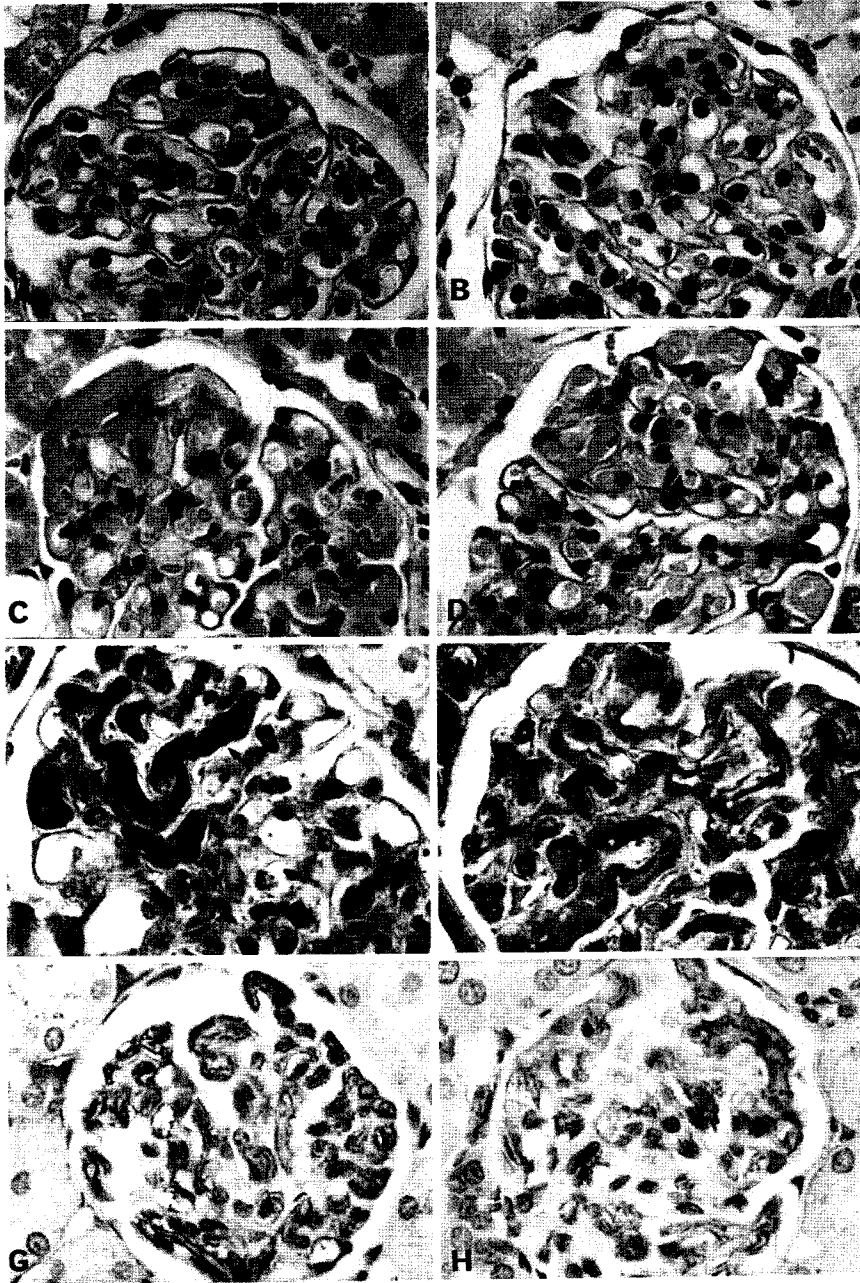


Fig. 5 Rat glomerulus after endotoxin (Et., 7.5 mg/kg) injection under the light microscope. A, Normal control. (HE staining, $\times 180$). B, Two hours after Et. injection. Edema in the capillaries is noted. (HE staining, $\times 180$). C, Four hours after Et. injection. Eosinophilic substances in the capillaries suggest fibrin thrombi. (HE staining, $\times 180$). D, Six hours after Et. injection, showing a reduction in eosin staining of fibrin thrombi. (HE staining, $\times 180$). E, Four hours after Et. injection. Fibriform structures (arrow) are observed in the fibrin thrombi. (PTAH staining, $\times 180$). F, Six hours after Et. injection, showing a reduction in PTAH staining and a decrease in fibriform structure. (PTAH staining, $\times 180$). G, Four hours after Et. injection, showing strongly positive fibrin thrombi in the capillaries. (ABC method for fibrinogen, $\times 180$). H, Six hours after Et. injection, showing a reduced reaction of fibrin thrombi for fibrinogen. (ABC method for fibrinogen, $\times 180$).

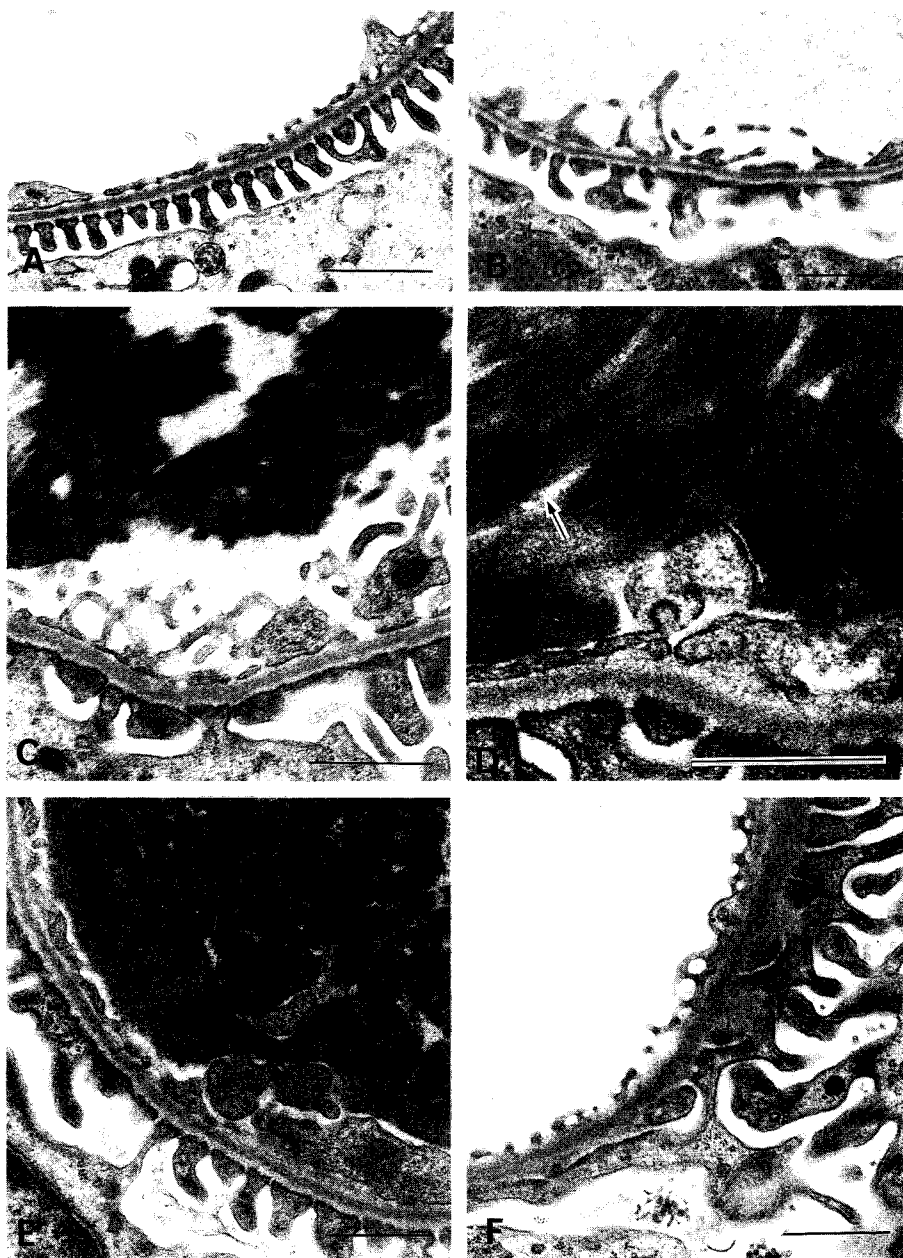


Fig. 6 Rat glomerular capillary and fibrin thrombus after endotoxin (Et., 7.5 mg/kg) injection under the transmission electron microscope. A, Capillary of a normal rat (group A), showing a regular arrangement of endothelial pores and foot processes of podocytes. B, Two hours after Et. injection, showing an irregular arrangement of endothelial pores and foot processes of podocytes. A fusion of foot processes is shown. C, Four hours after Et. injection, showing an increased number of irregular structures in the endothelial cytoplasm and fibrin thrombi composed of bundles of fibrin fibers. D, Four hours after Et. injection, showing a high power magnification of fibrin bundles. Cross-striated-structures of 20 nm (arrow) are clearly present. E, Six hours after Et. injection, showing a maculated fibrin thrombus. F, Twelve hours after Et. injection, showing restoration of the fine structure of the capillary. The edema of the basement membrane and foot processes, and fusion of the foot processes remain. Bars = 1 μ m; 80 kV.

Light microscopic findings. Fig. 5 shows changes in the glomeruli of Et. induced DIC rats. Under HE stain (Fig. 5B), edema was observed in the glomerular endothelium at 2 h after Et. injection. At 4 and 6 h, many glo-

merular capillaries with fibrin thrombi were observed. The fibrin thrombi disappeared at 12 h after Et. injection. The newly formed fibrin thrombi were strongly eosinophilic and had a fibrous structure under HE stain (Fig.

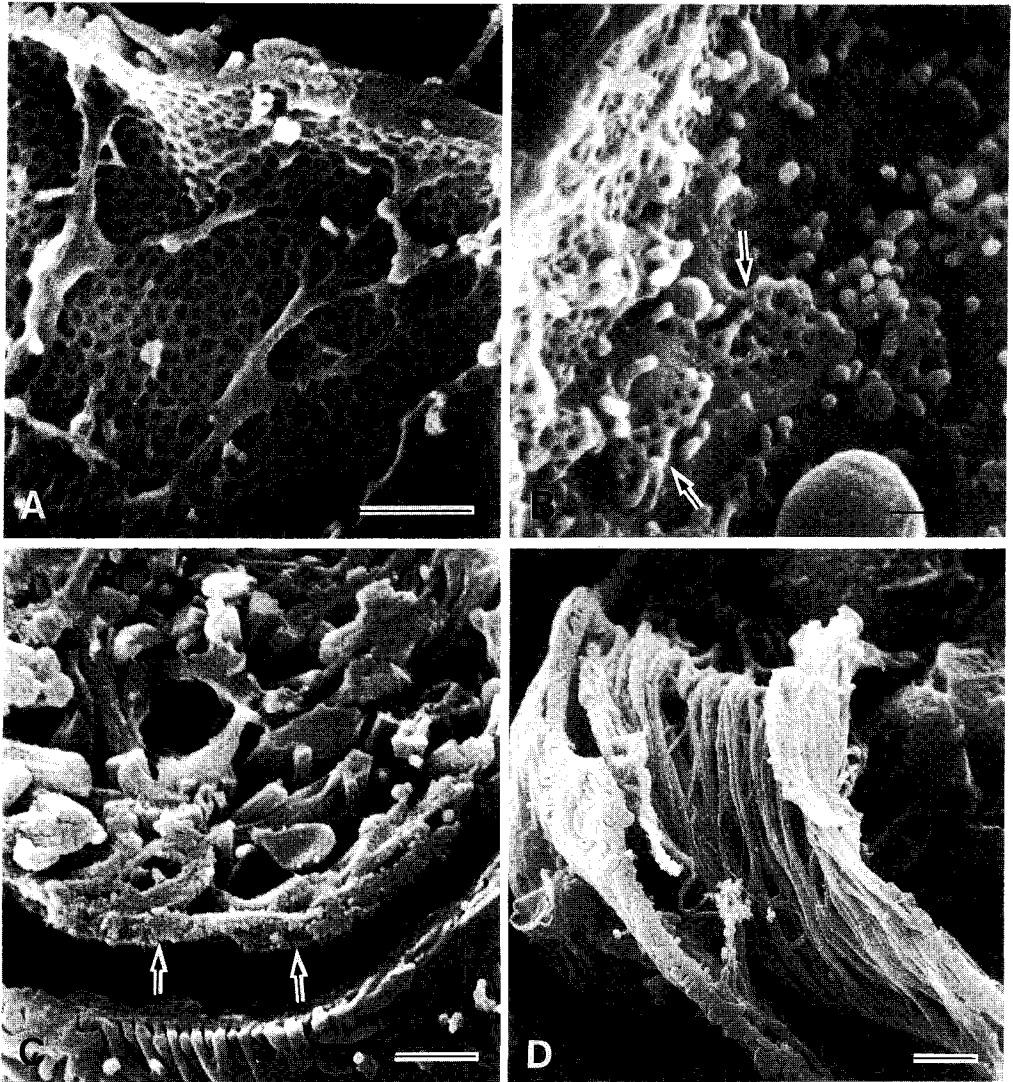


Fig. 7 Rat glomerular capillary and fibrin thrombus after endotoxin (Et., 7.5 mg/kg) injection under the scanning electron microscope. A, Capillary of a normal rat (group A) with regularly arranged endothelial pores. B, Two hours after Et. injection, showing an irregular arrangement of endothelial pores and projections with a sea anemone-like configuration. The arrow shows an exfoliated endothelial sheet. C, Four hours after Et. injection, showing fibrin fibers forming a bundle. The arrow shows a cross section of the bundles in a cracked dimension. D, Four hours after Et. injection, showing agglomerated long fibrin bundles consisting of long fibrin fibers in a non-cracked dimension.

5C). With the lapse of time, the eosinophilic hue decreased, and the fibrous structure changed to a colloidal appearance (Fig. 5D). Under PTAH stain, the fibrous structure was clearer than under HE stain at 4 h (Fig.

5E), but with time, the PTAH staining and structure of the thrombi became similar to the HE stained material at 6 h after Et. injection (Fig. 5F). The immunohistochemical reaction showed similar results to PTAH

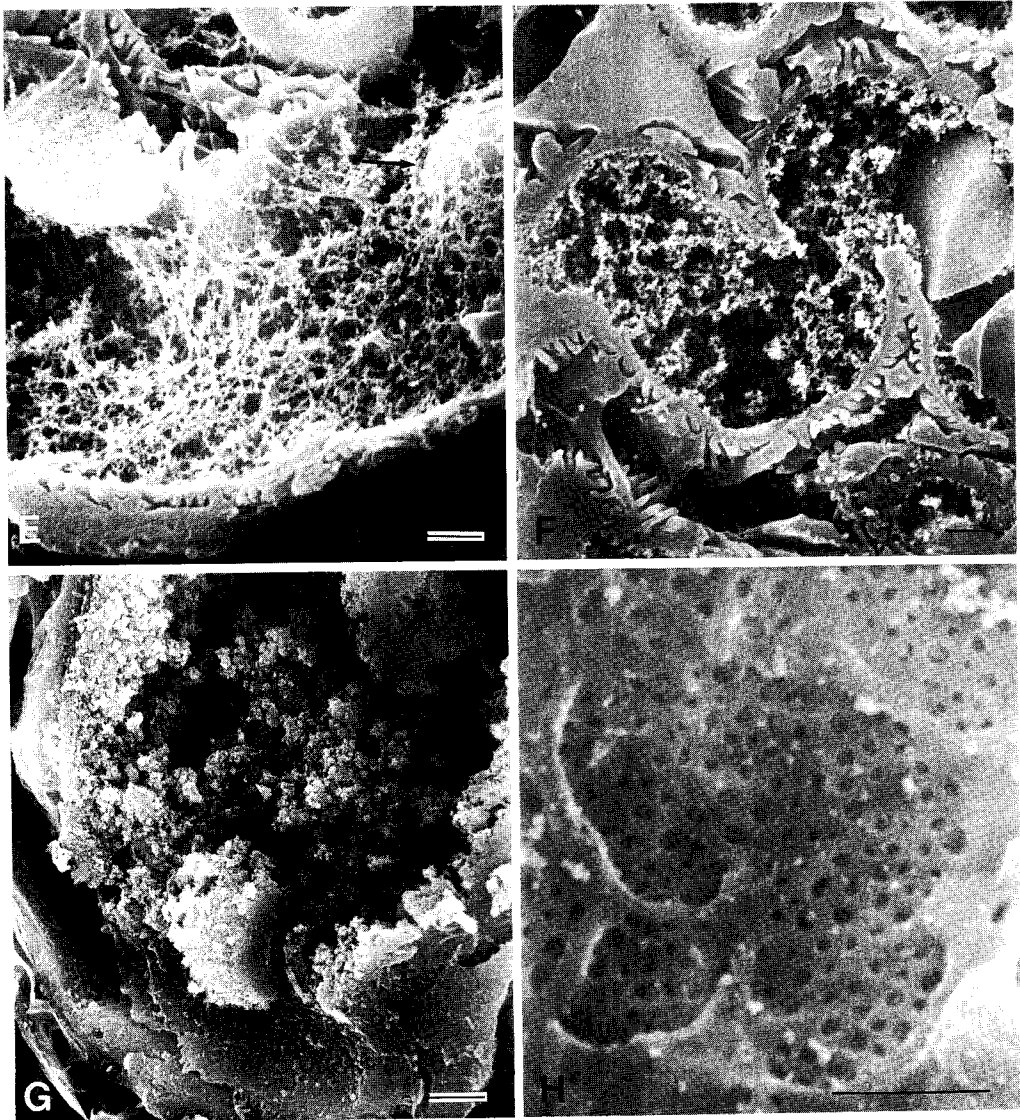


Fig. 7 Continued. E, Six hours after Et. injection, showing fibrin thrombus with a fine reticular configuration and firmly adhering to the endothelium. The arrow shows the reticular fibers of the fibrin thrombus covering a blood cell. F, Eight hours after Et. injection, showing a change in the reticular nest. The fibers agglomerate with one another, and the reticular configuration has disappeared. G, Eight hours after Et. injection, showing an agglomerated fibrin thrombus with a granular configuration. H, Twelve hours after Et. injection. The fibrin thrombus has disappeared, but the edema of endothelial cytoplasm remains. Bars = 1 μ m; 20 kV.

staining. There were strongly positive fibrin thrombi in the capillaries at 4 h, but they showed reduced reaction at 6 h after Et. injection (Fig. 5G, 5H).

Electron microscopic findings. Under TEM, the endothelial pores (120–150 nm in diameter) of the glomerular capillaries were regularly and evenly arranged on the surface of the basement membrane, and the foot processes of the podocyte were also regularly arranged with the same distances as the controls (Fig. 6A). At 2 h after Et. injection (Fig. 6B), the endothelial pores became irregular in arrangement and size, and were projected toward the lumen forming a tear drop configuration of 120–240 nm resulting in a sea anemone-like appearance. The foot processes of the podocytes were irregularly stretched, and sometimes fused with each other. However fibrin thrombi were not observed at this time. At 4 h after Et. injection (Fig. 6C, 6D), alterations in the endothelium and podocytes were accentuated. High contrast fibrin bundles of 120–240 nm were identified with fine cross-striated-fibrin structures at about 20 nm intervals. At 6 h after Et. injection (Fig. 6E), these fibrin bundles agglomerated with one another. They lost their bundle structure and acquired a maculous configuration of heterogenous electron density. At 12 h after Et. injection (Fig. 6F), all fibrin thrombi disappeared, but the irregularity of the endothelial surface and foot processes of the podocyte, and the edema of the basement membrane remained. These changes disappeared by 24 h after Et. injection.

Under SEM, endothelial surface of the glomerular capillary of the controls was smooth, and the endothelial pores were of the same size and evenly distributed (Fig. 7A). At 2 h after Et. injection (Fig. 7B), the capillary endothelium was very edematous and formed a number of tear-drop-like projections. The pores became irregular and

unevenly distributed. Sheet like exfoliations of endothelial cytoplasm were seen. Fibrin thrombi were not observed. At 4 h after Et. injection (Fig. 7C, 7D), thin fibrin fibers of 20–30 nm gathered, forming fibrin bundles of 120–240 nm in thickness. At 6 h after Et. injection (Fig. 7E), the bundle structure of the fibrin fibers disappeared, and the fibers acquired a fine reticular configuration and adhered tightly to the endothelial surface. With time, they agglomerated with one another (Fig. 7F). They showed a fine granular pattern at 8 h after Et. injection (Fig. 7G), and gradually decreased in number. The fibrin thrombi disappeared by 12 h after Et. injection, but the edema and irregularity of the capillary endothelial surface remained (Fig. 7H). The endothelial configuration returned to normal by 24 h after Et. injection.

Discussion

Et.-induced DIC models have been reported in the rabbit (17–19) and rat (20, 21). In these animals, the initiation, duration and target organ differed in accordance with the Et. dose and administration procedures. In our experiment, a dose of 7.5 mg/kg Et. was determined to be the LD₅₀ (Table 1), which is in agreement with the report of Berczi *et al.* (22). In group A animals, all biological and pathological findings such as blood platelet count (Fig. 1), serum and urinary FDP (Figs. 2, 3), urinary volume (Fig. 4), and fibrin thrombus formation in the glomerular capillary (Fig. 5) indicated DIC. Almost all rats administered an excessive dose of Et., died within 1 h. In these animals, the direct toxicity of Et. was probably the cause of death because fibrin thrombi were not observed in the glomerulus within 4 h of Et. injection (Table 1).

In man, DIC is a clinical entity followed

by various underlying etiologies. In causative studies, there have been a number of biochemical findings (23, 24), but TEM (12, 13) and especially SEM studies are rarely encountered. Our study is the first detailed study by TEM and SEM. Ultramicrostructural changes (Figs. 6, 7) illustrated the initiation, development and recovery processes of DIC. Coagulation on the endothelial surface (Fig. 7B) began upon initiation, and fibrin bundle formation (Figs. 7C, 7D) was observed during thrombosis, and fibrinolysis was observed upon degradation of fibrin thrombi (Figs. 7E-G). Prior to fibrin thrombus formation, the capillary endothelium was markedly injured as shown in Fig. 8B and Fig. 9B. Biochemical substances such as tissue thromboplastin were considered to be released from the injured endothelium, and fibrin thrombus formation was followed by an acceleration of coagulation (25). Then, fibrin fibers gathered together to form fibrin bundles (Figs. 7C, 7D), and agglomerated into a reticular pattern and firmly adhered to the endothelium (Fig. 7E). The injury to the surface of the capillary endothelium probably caused by direct effect of Et., which result in an irregular sea anemone-like appearance (Figs. 6B, 7B), would contribute to a decrease in blood flow and adhesion of the fibrin thrombus. The oliguria observed before fibrin thrombus formation could thus be due to the marked decrease in renal blood flow. As Furutani (26) has pointed out, ischemia of an organ might be an important prodromal factor in the initiation of DIC. We think that changes in the endothelial configuration (Fig. 7b) contribute to fibrin thrombus adhesion to the blood vessels, and to the development and maintenance of DIC. Thus, a fibrin thrombus is not formed *in situ* in the glomerular capillary, but precursors of the fibrin thrombus flow into the glomerular capillary, and form fibrin thrombi. This indicates that the DIC in our

study was caused by Et., but that fibrin thrombus formation and thrombus adhesion to the capillary had different causes. The former is due to biochemical substances, and the latter is due mainly to the microstructure of the renal tissue. Fibrin thrombi are frequently observed histologically in the glomerulus (2) probably because the renal glomerulus consists of a mass of capillaries with characteristic endothelial pores. These morphological characteristics are suitable for hemostasis and for the formation and adhesion of fibrin thrombi, and play the major role in the development and maintenance of the DIC state. Immunohistochemical findings (14) suggest that the term fibrin thrombus is not an exact term even at a relatively early stage. The fibrin thrombus is an admixture of fibrinogen, fibrin, FDP-D and FDP-E. This indicates that fibrin with fine reticular structure (Fig. 7E) are a complex of insoluble FDP of large molecular weight, fibrinogen, and fibrin polymer, and they gradually undergo degradation and become soluble substances of smaller molecular weight, and agglomerate into a granular configuration (Figs. 7F, 7G). Finally, they exit from the glomerulus and re-circulate (27) in the extrarenal vessels or are excreted into the urine through the Bowman's capsule and tubulus (Fig. 3) with or without biochemical changes (27, 28) as suggested by Kawasaki *et al.* (29) and Toyohuku *et al.* (15).

We conclude from our observations that injury to the capillary endothelium plays the main role in the initiation, development and maintenance of our Et.-induced DIC. However, it needs to be investigated whether or not there are differences in the initiation mechanism depending on the etiology.

Acknowledgements. The authors are indebted to Dr. C. L. Hsueh and Prof. S. Hibi for critical suggestions and discussion, and Dr. H. Yamamoto and Mrs. M. Takahashi for help with the operation of the transmission electron microscope.

References

1. Mckey DG: Disseminated intravascular coagulation; in *An Intermediary Mechanism of Disease*, Harper-Hoeber, New York (1965) pp 493-495.
2. Robby SJ, Colman RW and Minna JD: Pathology and disseminated intravascular coagulation (DIC): Analysis of twenty-six cases. *Hum Pathol* (1972) **3**, 327-343.
3. Hamilton PJ, Stalker AL and Doughras AS: Disseminated intravascular coagulation. *J Clin Pathol* (1978) **31**, 609-619.
44. Owen CA Jr and Bowie EJW: Chronic intravascular coagulation syndromes. *Mayo Clin Proc* (1974) **49**, 673-679.
5. Kazmier F, Bowie EJ, Hagedorn AB and Owen CA Jr: Treatment of intravascular coagulation and fibrinolysis (ICF) syndromes. *Mayo Clin Proc* (1974) **49**, 665-672.
6. Deyken D: The clinical challenge of disseminated intravascular coagulation. *N Engl J Med* (1970) **283**, 636-644.
7. Cooper HA, Bowie EJW and Owen CA Jr: Evaluation of patients with increased fibrinolytic split products (FSP) in their serum. *Mayo Clin Proc* (1974) **49**, 654-657.
8. Margaretten W: Damage in disseminated intravascular clotting. *Am J Cardiol* (1967) **20**, 185-190.
9. Lipinski B and Jeljaszewicz J: A hypothesis for the pathogenesis of the generalized Schwartzman reaction. *J Infect Dis* (1969) **20**, 160-168.
10. Hathaway WE, Belhasen LP and Hathaway HS: Evidence for a new plasma thromboplastin factor. *Blood* (1965) **26**, 521-532.
11. Saito H, Ratnoff OD, Waldmann R and Abraham JP: Fitzgerald trait. *J Clin Invest* (1975) **55**, 1082-1089.
12. Vassalli P, Simon G and Rouiller C: Electron microscopic study of glomerular lesions resulting from intravascular fibrin formation. *Am J Pathol* (1963) **43**, 579-617.
13. Bleyl U: Disseminated intravascular coagulation. *Semin Thromb Hemostasis* (1977) **3**, 247-267.
14. Ando T: An ultrastructural and cytochemical study of the rat kidney in experimentally induced endotoxin shock: *J Jpn Surg Soc* (1984) **85**, 835-848 (in Japanese).
15. Toyohuku H, Hayashi K and Awai M: An immunohistochemical study of experimental disseminated intravascular coagulation (DIC). *Acta Pathol Jpn* (1987) **37**, 1279-1290.
16. Craane H, Emeis JJ, Lindeman J and Nieuwenhuizen W: Immunoenzyme histochemical detection of fibrin microthrombi during disseminated intravascular coagulation in rats. *Histochemistry* (1978) **57**, 97-105.
17. Watanabe T and Tanaka K: An electron microscopic observation of the kidney in the generalized Schwartzman reaction; in *Topics in Hematology*, Seno, Takaku and Irino eds, Excerpta Medica, Amsterdam-Oxford (1977) pp 775-778.
18. Mckey DG, Gitlin D and Craig JM: Immunochemical demonstration of fibrin in the generalized Schwartzman reaction. *Arch Pathol* (1959) **67**, 270-282.
19. Beller FK: The role of endotoxin in disseminated intravascular coagulation; in *Disseminated Intravascular Coagulation*, Schattauer FK Schattauer Verlag, Stuttgart-New York (1969) pp 125-138.
20. Schoendorf TH, Rosenberg M and Beller FK: Endotoxin-induced disseminated intravascular coagulation in nonpregnant rats. *Am J Pathol* (1971) **65**, 51-58.
21. Emeis JJ, Lindeman J and Nieuwenhuizen W: Immunoenzyme histochemical localization of fibrin degradation products in tissues. *Am J Pathol* (1981) **103**, 337-344.
22. Berczi I, Bretok L and Bereznai T: Comparative studies on the toxicity of *Escherichia coli* lipopolysaccharide endotoxin in various animal species. *Can J Microbiol* (1966) **12**, 1070-1079.
23. Hardaway RM: Coagulation factors in shock; in *Shock-Metabolic Disorders and Therapy*, Zimmermann ed, Vol 1, Schattauer Verlag, Stuttgart-New York (1972) pp 409-413.
24. Hathaway WE, Belhasen LP and Hathaway HS: Evidence for a new plasma thromboplastin factor. *Blood* (1965) **26**, 521-532.
25. Kaplan JE and Saba TM: Low grade intravascular coagulation and reticuloendothelial function. *Am Phys Soc* (1978) **52**, 323-328.
26. Furutani S: Histopathological study of acute renal failure (ARF). Course of histopathologic changes in experimental ischemic kidney. *Okayama Igakkai Zasshi* (1984) **96**, 791-813 (in Japanese).
27. Wintrobe MM: *Clinical Hematology*. Leu and Fibriger, Philadelphia (1974) pp 1201-1232.
28. Sherman LA: *In vitro* formation and *in vivo* clearance of fibrinogen and fibrin complexes. *J Lab Clin Med* (1975) **86**, 100-111.
29. Kawasaki H, Hayashi K and Awai M: Disseminated intravascular coagulation; Immunohistochemical study of fibrin-related materials (FRMs) in renal tissues. *Acta Pathol Jpn* (1987) **37**, 77-84.

Received January 9, 1989; accepted February 7, 1989